

Gravastars with Dark Energy Evolving to Naked Singularity

R. Chan ^{1,*} M.F.A. da Silva ^{2,†} P. Rocha ^{2,3,‡} and J.F. Villas da Rocha ^{4§}

¹ *Coordenação de Astronomia e Astrofísica,*

Observatório Nacional, Rua General José Cristino, 77,

São Cristóvão, 20921-400, Rio de Janeiro, RJ, Brazil

² *Departamento de Física Teórica, Instituto de Física,*

Universidade do Estado do Rio de Janeiro,

Rua São Francisco Xavier 524, Maracanã,

20550-900, Rio de Janeiro - RJ, Brasil

³ *IST - Instituto Superior de Tecnologia de Paracambi,*

FAETEC, Rua Sebastião de Lacerda s/n,

Bairro da Fábrica, Paracambi, 26600-000, RJ, Brazil

⁴ *Universidade Federal do Estado do Rio de Janeiro,*

Instituto de Biociências, Departamento de Ciências Naturais,

Av. Pasteur 458, Urca, 22290-240, Rio de Janeiro, RJ, Brazil

(Dated: September 28, 2018)

Abstract

We consider a gravastar model made of anisotropic dark energy with an infinitely thin spherical shell of a perfect fluid with the equation of state $p = (1 - \gamma)\sigma$ with an external de Sitter-Schwarzschild region. It is found that in some cases the models represent the "bounded excursion" stable gravastars, where the thin shell is oscillating between two finite radii, while in other cases they collapse until the formation of black holes or naked singularities. An interesting result is that we can have black hole and stable gravastar formation even with an interior and a shell constituted of dark and repulsive dark energy, as also shown in previous work. Besides, in three cases we have a dynamical evolution to a black hole (for $\Lambda = 0$) or to a naked singularity (for $\Lambda > 0$). This is the first time in the literature that a naked singularity emerges from a gravastar model.

PACS numbers: 98.80.-k,04.20.Cv,04.70.Dy

*Electronic address: chan@on.br

[†]Electronic address: mfasnic@gmail.com

[‡]Electronic address: pedrosennarocho@gmail.com

[§]Electronic address: jfvroch@pq.cnpq.br

I. INTRODUCTION

As alternatives to black holes, gravastars have received some attention recently [1], partially due to the tight connection between the cosmological constant and a currently accelerating universe [2], although very strict observational constraints on the existence of such stars may exist [3].

The pioneer model of gravastar was proposed by Mazur and Mottola (MM) [4], consisting of five layers: an internal core $0 < R < R_1$, described by the de Sitter universe, an intermediate thin layer of stiff fluid $R_1 < R < R_2$, an external region $R > R_2$, described by the Schwarzschild solution, and two infinitely thin shells, appearing, respectively, on the hypersurfaces $R = R_1$ and $R = R_2$. The intermediate layer is constructed in such way that R_1 is inner than the de Sitter horizon, while R_2 is outer than the Schwarzschild horizon, eliminating the apparent horizon. Configurations with a de Sitter interior have long history which we can find, for example, in the work of Dymnikova and Galaktionov [5]. After this work, Visser and Wiltshire [6] pointed out that there are two different types of stable gravastars which are stable gravastars and “bounded excursion” gravastars. In the spherically symmetric case, the motion of the surface of the gravastar can be written in the form [6],

$$\frac{1}{2}\dot{R}^2 + V(R) = 0, \quad (1)$$

where R denotes the radius of the star, and $\dot{R} \equiv dR/d\tau$, with τ being the proper time of the surface. Depending on the properties of the potential $V(R)$, the two kinds of gravastars are defined as follows.

Stable gravastars: In this case, there must exist a radius R_0 such that

$$V(R_0) = 0, \quad V'(R_0) = 0, \quad V''(R_0) > 0, \quad (2)$$

where a prime denotes the ordinary differentiation with respect to the indicated argument. If and only if there exists such a radius R_0 for which the above conditions are satisfied, the model is said to be stable. Among other things, VW found that there are many equations of state for which the gravastar configurations are stable, while others are not [6]. Carter studied the same problem and found new equations of state for which the gravastar is stable [7], while De Benedictis *et al* [8] and Chirenti and Rezzolla [9] investigated the stability of the original model of Mazur and Mottola against axial-perturbations, and found that

gravastars are stable to these perturbations, too. Chirenti and Rezzolla also showed that their quasi-normal modes differ from those of black holes with the same mass, and thus can be used to discern a gravastar from a black hole.

”Bounded excursion” gravastars: As VW noticed, there is a less stringent notion of stability, the so-called “bounded excursion” models, in which there exist two radii R_1 and R_2 such that

$$V(R_1) = 0, \quad V'(R_1) \leq 0, \quad V(R_2) = 0, \quad V'(R_2) \geq 0, \quad (3)$$

with $V(R) < 0$ for $a \in (R_1, R_2)$, where $R_2 > R_1$.

Lately, we studied both types of gravastars [10, 11], and found that, such configurations can indeed be constructed, although the region for the formation of them is very small in comparison to that of black holes.

Based on the discussions about the gravastar picture some authors have proposed alternative models [15]. Among them, we can find a Chaplygin dark star [16], a gravastar supported by non-linear electrodynamics [17], a gravastar with continuous anisotropic pressure [18] and recently, Dzhunushaliev et al. worked on spherically symmetric configurations of a phantom scalar field and they found something like a gravastar but it was unstable [19]. In addition, Lobo [20] studied two models for a dark energy fluid. One of them describes a homogeneous energy density and the other describes an ad-hoc monotonically decreasing energy density, although both of them are with anisotropic pressure. In order to match an exterior Schwarzschild spacetime he introduced a thin shell between the interior and the exterior spacetimes.

In this paper, we generalize our previous works [10, 11] to the case where the equation of state of the infinitely thin shell is given by $p = (1 - \gamma)\sigma$ with γ being a constant, the interior consists of a phantom energy fluid [20], while the exterior is still the Schwarzschild space. We shall first construct three-layer dynamical models, and then show both types of gravastars and black holes exist for various situations. The rest of the paper is organized as follows: In Sec. II we present the metrics of the interior and exterior spacetimes, and write down the motion of the thin shell in the form of equation (1). In Sec. III we show the definitions of dark and phantom energy, for the interior fluid and for the shell. In Sec. IV we discuss the formation of black holes from standard or phantom energy. In Sec. V we analyze the formation of gravastar or normal star from standard or phantom energy. In Sec. VI we study special cases where we can not have the ”bounded excursion”. Finally, in Sec.

VII we present our conclusions.

II. DYNAMICAL THREE-LAYER PROTOTYPE GRAVASTARS

The interior fluid is made of an anisotropic dark energy fluid with a metric given by [20]

$$ds_-^2 = -f_1 dt^2 + f_2 dr^2 + r^2 d\Omega^2, \quad (4)$$

where $d\Omega^2 \equiv d\theta^2 + \sin^2(\theta)d\phi^2$, and

$$\begin{aligned} f_1 &= (1 + br^2)^{\frac{1-\omega}{2}} (1 + 2br^2)^\omega, \\ f_2 &= \frac{1 + 2br^2}{1 + br^2}, \end{aligned} \quad (5)$$

where ω is a constant, and its physical meaning can be seen from the following equation (6). Since the mass is given by $\bar{m}(r) = br^3/[2(1 + 2br^2)]$ then we have that $b > 0$. The corresponding energy density ρ , radial and tangential pressures p_r and p_t are given, respectively, by

$$\begin{aligned} p_r &= \omega\rho = \left(\frac{\omega b}{8\pi}\right) \left(\frac{3 + 2br^2}{(1 + 2br^2)^2}\right), \\ p_t &= -\left(\frac{b}{8\pi}\right) \left(\frac{\omega(3 + 2br^2)}{(1 + 2br^2)^2}\right) + \frac{b^2 r^2}{32\pi [(1 + 2br^2)^3(1 + br^2)]} \times \\ &\quad \left\{ (1 + \omega)(3 + 2br^2) [(1 + 3\omega) + 2br^2(1 + \omega)] \right. \\ &\quad \left. - 8\omega(5 + 2br^2)(1 + br^2) \right\}. \end{aligned} \quad (6)$$

The exterior spacetime is given by the Schwarzschild metric

$$ds_+^2 = -fdv^2 + f^{-1}d\mathbf{r}^2 + \mathbf{r}^2 d\Omega^2, \quad (7)$$

where $f = 1 - 2m/\mathbf{r} - (\mathbf{r}/L_e)^2$ and $L_e = \sqrt{3/\Lambda_e}$. The metric of the hypersurface on the shell is given by

$$ds_\Sigma^2 = -d\tau^2 + R^2(\tau)d\Omega^2. \quad (8)$$

Since $ds_-^2 = ds_+^2 = ds_\Sigma^2$, we find that $r_\Sigma = \mathbf{r}_\Sigma = R$, and

$$f_1 \dot{t}^2 - f_2 \dot{R}^2 = 1, \quad (9)$$

$$f \dot{v}^2 - \frac{\dot{R}^2}{f} = 1, \quad (10)$$

where the dot denotes the ordinary differentiation with respect to the proper time. On the other hand, the interior and exterior normal vectors to the thin shell are given by

$$\begin{aligned} n_{\alpha}^{-} &= (-\dot{R}, \dot{t}, 0, 0), \\ n_{\alpha}^{+} &= (-\dot{R}, \dot{v}, 0, 0). \end{aligned} \quad (11)$$

Then, the interior and exterior extrinsic curvature are given by

$$\begin{aligned} K_{\tau\tau}^i &= \frac{1}{2}(1 + bR^2)^{-\omega/2}\dot{t} \left\{ \left[4(1 + bR^2)^{\omega/2}bR^2\dot{R}^2 + 2(1 + bR^2)^{\omega/2}\dot{R}^2 - \right. \right. \\ &\quad \left. \left. (1 + 2bR^2)^{\omega}\sqrt{1 + bR^2}bR^2\dot{t}^2 - (1 + 2bR^2)^{\omega}\sqrt{1 + bR^2}\dot{t}^2 \right] (2bR^2\omega + 2bR^2 + 3\omega + 1) - \right. \\ &\quad \left. 2(1 + bR^2)^{\omega/2}(1 + 2bR^2)\dot{R}^2 \right\} (1 + 2bR^2)^{-2}(1 + bR^2)^{-1}bR + \dot{R}\ddot{t} - \ddot{R}\dot{t}, \end{aligned} \quad (12)$$

$$(13)$$

$$K_{\theta\theta}^i = \frac{\dot{t}(1 + bR^2)R}{1 + 2bR^2}, \quad (14)$$

$$K_{\phi\phi}^i = K_{\theta\theta}^{-} \sin^2(\theta), \quad (15)$$

$$\begin{aligned} K_{\tau\tau}^e &= \dot{v}[(2L_e^2m\dot{v} + L_e^2R\dot{R} - L_e^2R\dot{v} + R^3\dot{v})(2L_e^2m\dot{v} - L_e^2R\dot{R} - L_e^2R\dot{v} + R^3\dot{v}) - \\ &\quad 2L_e^4R^2\dot{R}^2][(2m - R)L_e^2 + R^3]^{-1}(L_e^2m - R^3)L_e^{-4}R^{-3} + \dot{R}\ddot{v} - \ddot{R}\dot{v} \end{aligned} \quad (16)$$

$$K_{\theta\theta}^e = -\dot{v}((2m - R)L_e^2 + R^3)L_e^{-2} \quad (17)$$

$$K_{\phi\phi}^e = K_{\theta\theta}^e \sin^2(\theta). \quad (18)$$

Since [21]

$$[K_{\theta\theta}] = K_{\theta\theta}^e - K_{\theta\theta}^i = -M, \quad (19)$$

where M is the mass of the shell, we find that

$$M = \dot{v}(2m - R) + \frac{\dot{t}(1 + bR^2)R}{1 + 2bR^2}. \quad (20)$$

Then, substituting equations (9) and (10) into (20) we get

$$M = -R \left(1 - \frac{2m}{R} - \left(\frac{R}{L_e} \right)^2 + \dot{R}^2 \right)^{1/2} + R \frac{\left[1 + bR^2 + \dot{R}^2(1 + 2bR^2) \right]^{1/2}}{(1 + bR^2)^{-(\omega+1)/4}(1 + 2bR^2)^{(\omega+2)/2}}. \quad (21)$$

In order to keep the ideas of MM as much as possible, we consider the thin shell as consisting of a fluid with the equation of state, $p = (1 - \gamma)\sigma$, where σ and p denote, respectively, the

surface energy density and pressure of the shell and γ is a constant. Then, the equation of motion of the shell is given by [21]

$$\dot{M} + 8\pi R\dot{R}p = 4\pi R^2[T_{\alpha\beta}u^\alpha n^\beta] = 4\pi R^2\left(T_{\alpha\beta}^e u_e^\alpha n_e^\beta - T_{\alpha\beta}^i u_i^\alpha n_i^\beta\right), \quad (22)$$

where u^α is the four-velocity. Since the interior fluid is made of an anisotropic fluid and the exterior is vacuum, we get

$$\dot{M} + 8\pi R\dot{R}(1 - \gamma)\sigma = 0. \quad (23)$$

Recall that $\sigma = M/(4\pi R^2)$, we find that equation (23) has the solution

$$M = kR^{2(\gamma-1)}, \quad (24)$$

where k is an integration constant. Substituting equation (24) into equation (21), and rescaling m , b and R as,

$$\begin{aligned} m &\rightarrow mk^{-\frac{1}{2\gamma-3}}, \\ b &\rightarrow bk^{\frac{2}{2\gamma-3}}, \\ R &\rightarrow Rk^{-\frac{1}{2\gamma-3}}, \end{aligned} \quad (25)$$

we find that it can be written in the form of equation (1), and

$$\begin{aligned} V(R, m, L_e, \omega, b, \gamma) = &-\frac{1}{2L_e^2 R^2 b_2 \left(b_2^{\omega+1} b_1^{-\frac{1}{2}\omega} - b_1^{\frac{1}{2}}\right)^2} (b_2^{2\omega+3} R^{4\gamma-4} b_1^{-\omega} L_e^2 \\ &- 2b_1^{-\frac{1}{2}\omega+\frac{1}{2}} R^{2\gamma-2} b_2^{\omega+1} L_e (-b_2 (b_2^{\omega+2} b_1^{-\frac{1}{2}\omega} R^6 L_e^2 - 2b_2^{\omega+2} b_1^{-\frac{1}{2}\omega} m L_e^2 R^5 - \\ &b_2^{\omega+2} b_1^{-\frac{1}{2}\omega} R^8 - b_2^{\omega+1} b_1^{-\frac{1}{2}\omega+1} R^6 L_e^2 - R^6 L_e^2 b_2 b_1^{\frac{1}{2}} + 2m L_e^2 b_2 R^5 b_1^{\frac{1}{2}} + \\ &R^8 b_2 b_1^{\frac{1}{2}} + R^6 L_e^2 b_1^{\frac{3}{2}} - b_2^{\omega+2} L_e^2 b_1^{-\frac{1}{2}\omega} R^{4\gamma}) / (b_1^{1/2} R^4))^{\frac{1}{2}} + b_1^{\frac{3}{2}-\frac{1}{2}\omega} b_2^{\omega+1} R^2 L_e^2 - \\ &b_1^2 R^2 L_e^2 + b_2^{\omega+2} b_1^{-\frac{1}{2}\omega+\frac{1}{2}} L_e^2 R^{4\gamma-4} - b_2^{2\omega+3} L_e^2 b_1^{-\omega} R^2 + b_2^{\omega+2} b_1^{-\frac{1}{2}\omega+\frac{1}{2}} R^2 L_e^2 + \\ &2b_2^{2\omega+3} b_1^{-\omega} R m L_e^2 - 2b_2^{\omega+2} b_1^{-\frac{1}{2}\omega+\frac{1}{2}} m L_e^2 R + b_2^{2\omega+3} b_1^{-\omega} R^4 - b_2^{\omega+2} b_1^{-\frac{1}{2}\omega+\frac{1}{2}} R^4) \end{aligned} \quad (26)$$

where

$$b_1 \equiv 1 + bR^2, \quad b_2 \equiv 1 + 2bR^2. \quad (27)$$

The exterior horizons are given by [24]

$$r_{bh} = \frac{2m}{\sqrt{3y}} \cos\left(\frac{\pi + \psi}{3}\right), \quad (28)$$

$$r_c = \frac{2m}{\sqrt{3y}} \cos\left(\frac{\pi - \psi}{3}\right), \quad (29)$$

where $y = (m/L_e)^2$, $\psi = \arccos(3\sqrt{3y})$, r_{bh} denotes the black hole horizon and r_c denotes the cosmological horizon. Note that if $y > 1/27$ the quantity $3\sqrt{3y}$ is greater than 1, giving an imaginary angle ψ . Thus, the horizons r_{bh} and r_c are imaginary and the spacetime becomes free of horizons.

To guarantee that initially the spacetime does not have any kind of horizons, cosmological or event, we must restrict R_0 to the range,

$$r_{bh} < R_0 < r_h \text{ or } r_c, \quad (30)$$

where R_0 is the initial collapse radius. Clearly, for any given constants m , ω , b and γ , equation (26) uniquely determines the collapse of the prototype gravastar. Depending on the initial value R_0 , the collapse can form either a black hole, a gravastar, a Minkowski, or a spacetime filled with phantom fluid. In the last case, the thin shell first collapses to a finite non-zero minimal radius and then expands to infinity. To guarantee that initially the spacetime does not have any kind of horizons, cosmological or event, we must restrict R_0 to the range,

$$R_0 > 2m, \quad (31)$$

where R_0 is the initial collapse radius. When $m = 0 = b$, the thin shell disappears, and the whole spacetime is Minkowski. So, in the following we shall not consider this case.

Since the potential (26) is so complicated, it is too difficult to study it analytically. Instead, in the following we shall study it numerically. Before doing so, we shall show the classifications of matter, dark energy, and phantom energy for anisotropic fluids.

III. CLASSIFICATIONS OF MATTER, DARK ENERGY, AND PHANTOM ENERGY FOR ANISOTROPIC FLUIDS

Recently [23], the classification of matter, dark and phantom energy for an anisotropic fluid was given in terms of the energy conditions. Such a classification is necessary for systems where anisotropy is important, and the pressure components may play very important roles and can have quite different contributions. In this paper, we will use this classification to study the collapse of the dynamical prototype gravastars, constructed in the last section.

TABLE I: This table summarizes the classification of the interior matter field, based on the energy conditions [22], where we assume that $\rho \geq 0$.

Matter	Condition 1	Condition 2	Condition 3
Normal Matter	$\rho + p_r + 2p_t \geq 0$	$\rho + p_r \geq 0$	$\rho + p_t \geq 0$
Dark Energy	$\rho + p_r + 2p_t < 0$	$\rho + p_r \geq 0$	$\rho + p_t \geq 0$
Repulsive Phantom Energy	$\rho + p_r + 2p_t < 0$	$\rho + p_r < 0$	$\rho + p_t \geq 0$
		$\rho + p_r \geq 0$	$\rho + p_t < 0$
Attractive Phantom Energy	$\rho + p_r + 2p_t \geq 0$	$\rho + p_r < 0$	$\rho + p_t < 0$
		$\rho + p_r \geq 0$	$\rho + p_t \geq 0$

TABLE II: This table summarizes the classification of matter on the thin shell, based on the energy conditions [22]. The last column indicates the particular values of the parameter γ , where we assume that $\rho \geq 0$.

Matter	Condition 1	Condition 2	γ
Normal Matter	$\sigma + 2p \geq 0$	$\sigma + p \geq 0$	-1 or 0
Dark Energy	$\sigma + 2p < 0$	$\sigma + p \geq 0$	7/4
Repulsive Phantom Energy	$\sigma + 2p < 0$	$\sigma + p < 0$	3

In particular, we define dark energy as a fluid which violates the strong energy condition (SEC). From the Raychaudhuri equation, we can see that such defined dark energy always exerts divergent forces on time-like or null geodesics. On the other hand, we define phantom energy as a fluid that violates at least one of the null energy conditions (NEC's). We shall further distinguish phantom energy that satisfies the SEC from that which does not satisfy the SEC. We call the former attractive phantom energy, and the latter repulsive phantom energy. Such a classification is summarized in Table I.

For the sake of completeness, in Table II we apply it to the matter field located on the thin shell, while in Table III we combine all the results of Tables I and II, and present all the possibilities.

In order to consider the equations (4) and (6) for describing dark energy stars we must

analyze carefully the ranges of the parameter ω that in fact furnish the expected fluids. It can be shown that the condition $\rho + p_r > 0$ is violated for $\omega < -1$ and fulfilled for $\omega > -1$, for any values of R and b . The conditions $\rho + p_t > 0$ and $\rho + p_r + 2p_t > 0$ are satisfied for $\omega < -1$ and $-1/3 < \omega < 0$, for any values of R and b . For the other intervals of ω the energy conditions depend on very complicated relations of R and b . See reference [23]. This provides an explicit example, in which the definition of dark energy must be dealt with great care. Another case was provided in a previous work [23]. Taking several values of ω in the intervals $-1 < \omega < -1/3$ and $\omega > 0$, we could not find any case where the interior dark energy exist.

In order to fulfill the energy condition $\sigma + 2p \geq 0$ of the shell and assuming that $p = (1 - \gamma)\sigma$ we must have $\gamma \leq 3/2$. On the other hand, in order to satisfy the condition $\sigma + p \geq 0$, we obtain $\gamma \leq 2$. Hereinafter, we will use only some particular values of the parameter γ which are analyzed in this work. See Table II.

IV. STRUCTURES FORMED

Here we can find many types of systems, depending on the combination of the constitution matter of the shell and core. Among them, there are formation of black holes, stable and "bounded excursion" gravastars, as it has already shown in our previous works [10]-[14], and even a naked singularity constituted exclusively of dark energy. All of them are listed in the table III.

As can be seen in the figures 1, 3 and 5, depending on the value of the cosmological constant, we can see that $V(R) = 0$ now can have one, two or three real roots. Then, we have, say, R_i , where $R_{i+1} > R_i$. For $L_e = L_1$ (corresponding to $\Lambda = 0$) If we choose $R_0 > R_3$ none structure is allowed in this region because the potential is greater than the zero. However, if we choose $R_2 < R_0 < R_3$, the collapse will bounce back and forth between $R = R_1$ and $R = R_2$. This is exactly the so-called "bounded excursion" model mentioned in [6], and studied in some details in [10]-[14]. Of course, in a realistic situation, the star will emit both gravitational waves and particles, and the potential will be self-adjusted to produce a minimum at $R = R_{static}$ where $V(R = R_{static}) = 0 = V'(R = R_{static})$ whereby a gravastar is finally formed [6, 10–12]. For $R_0 < R_1$ a black hole is formed in the end of the collapse of the shell.

The scenario above can significantly be changed if we consider $\Lambda > 0$. In this case for $L_e > L_c$, we also have bounded excursion gravastars if $R_2 < R_0 < R_3$. However, for $R_0 < R_1$ the final structure can be now a black hole or a naked singularity since the presence of the cosmological constant above a certain limit (L_e^*) eliminates the event horizon (its radius becomes imaginary), as can be seen in the tables IV, V and VI. This is the first evidence of a naked singularity formation from a gravastar model. Moreover for $L_e = L_c$, then $R_2 = R_3$, a stable gravastar is formed if $R_0 = R_2$, while for $L_e < L_c$ there is only one real root. Note that for any value of $L_e > L_e^*$, a naked singularity is formed for small initial radius of the shell. This is already present in the de Sitter-Schwarzschild solution [24], since is the exterior cosmological constant which allows to relax the inevitability of the horizon formation (differently from the Schwarzschild solution). The news here are that we have found a source (the shell with an interior anisotropic dark energy fluid) which can be matched with the de Sitter-Schwarzschild vacuum spacetime and, depending on the values of the exterior cosmological constant and the total mass, can represent a naked singularity.

Thus, solving equation (21) for $\dot{R}(\tau)$ we can integrate $\dot{R}(\tau)$ and obtain $R(\tau)$, which are shown in the figures 2, 4 and 6 for the case G.

V. CONCLUSIONS

In this paper, we have studied the problem of the stability of gravastars by constructing dynamical three-layer models of VW [6], which consists of an internal anisotropic dark energy fluid, a dynamical infinitely thin shell of perfect fluid with the equation of state $p = (1 - \gamma)\sigma$, and an external de Sitter-Schwarzschild spacetime.

We have shown explicitly that the final output can be a black hole, a "bounded excursion" stable gravastar depending on the total mass m of the system, the cosmological constant L_e , the parameter ω , the constant b , the parameter γ and the initial position R_0 of the dynamical shell. All these possibilities have non-zero measurements in the phase space of m , L_e , b , ω , γ and R_0 . All the results can be summarized in Table III.

An interesting result that we can deduce from Table III is that we can have black hole and stable gravastar formation even with an interior and a shell constituted of dark and repulsive dark energy (cases H and I). Still more interesting is the case G, represented by figures 1, 3 and 5 where for small radius of the shell we have no formation of a black hole

TABLE III: This table summarizes all possible kind of energy of the interior fluid and of the shell and compares the formed structures in the two gravastar models ($\Lambda_e = 0$, $\Lambda_e > 0$). The letters SG, UG, BEG, BH, NS and N denote stable gravastar, unstable gravastar, bounded excursion gravastar, black hole, naked singularity and none, respectively.

Case	Interior Energy	Shell Energy	Figures	Structures ($\Lambda_e = 0$)	Structures ($\Lambda_e > 0$)
A	Standard	Standard		SG	SG/UG/BEG
B	Standard	Dark		BH	SG/UG/BEG
C	Standard	Repulsive Phantom		BH	BH
D	Dark	Standard		N	N
E	Dark	Dark		N	N
F	Dark	Repulsive Phantom		N	N
G	Repulsive Phantom	Standard	1, 3, 5	SG/BEG	BH/SG/UG/BEG/NS
H	Repulsive Phantom	Dark		BH	BH/SG/UG/BEG
I	Repulsive Phantom	Repulsive Phantom		BH	BH
J	Attractive Phantom	Standard		SG/BEG	BH/SG/BEG
K	Attractive Phantom	Dark		BH	BH
L	Attractive Phantom	Repulsive Phantom		BH	BH

(for $\Lambda = 0$) and a naked singularity (for $\Lambda > 0$). This is the first time in the literature that a naked singularity emerges from a gravastar model. Besides, the figures 2, 4 and 6 give us examples of the dynamical evolution of a gravastar to a naked singularity.

Finally, the opposite final fates, because of the absence or the presence of a positive cosmological constant, reinforces the hypothesis proposed in [25] that can exist a connection between naked singularities and some kind of weakness of the gravitational field, compared to that associated to black holes.

Acknowledgments

The financial assistance from FAPERJ/UERJ (MFAdaS) are gratefully acknowledged. The authors (RC, MFAdaS, JFVR) acknowledges the financial support from FAPERJ (no. E-26/171.754/2000, E-26/171.533/2002, E-26/170.951/2006, E-26/110.432/2009 and

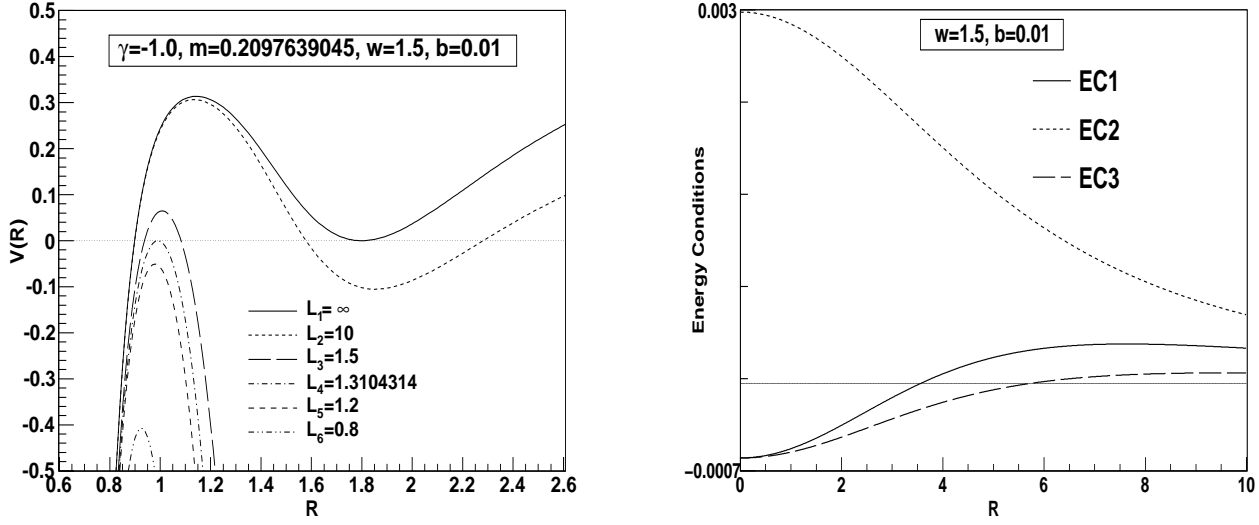


FIG. 1: The potential $V(R)$ and the energy conditions $EC1 \equiv \rho + p_r + 2p_t$, $EC2 \equiv \rho + p_r$ and $EC3 \equiv \rho + p_t$, for $\gamma = -1$, $\omega = 1.5$, $b = 0.01$ and $m_c = 0.2097639045$. **Case G**

TABLE IV: This table show the calculated horizons using the equations 28 and 29. The symbol $i = \sqrt{-1}$ denotes the imaginary constant. See figure 1.

m	L_e	Cosmological Horizon	Black Hole Horizon
0.2097639045	0.8	0.4795669330+0.2235024144 i	0.4795669330-0.2235024144 i
	L_e^*		
	1.2	0.8577020327	0.5136246691
	1.3104314	0.9974942529	0.4866382631
	1.5	1.213250267	0.4638970952
	10	9.783239233	0.4202701210
	∞	∞	$2m=0.4195278090$

E26/111.714/2010). The authors (RC, MFAdaS and JFVdR) also acknowledge the financial support from Conselho Nacional de Desenvolvimento Científico e Tecnológico - CNPq - Brazil (no. 450572/2009-9, 301973/2009-1 and 477268/2010-2). The author (MFAdaS) also acknowledges the financial support from Financiadora de Estudos e Projetos - FINEP

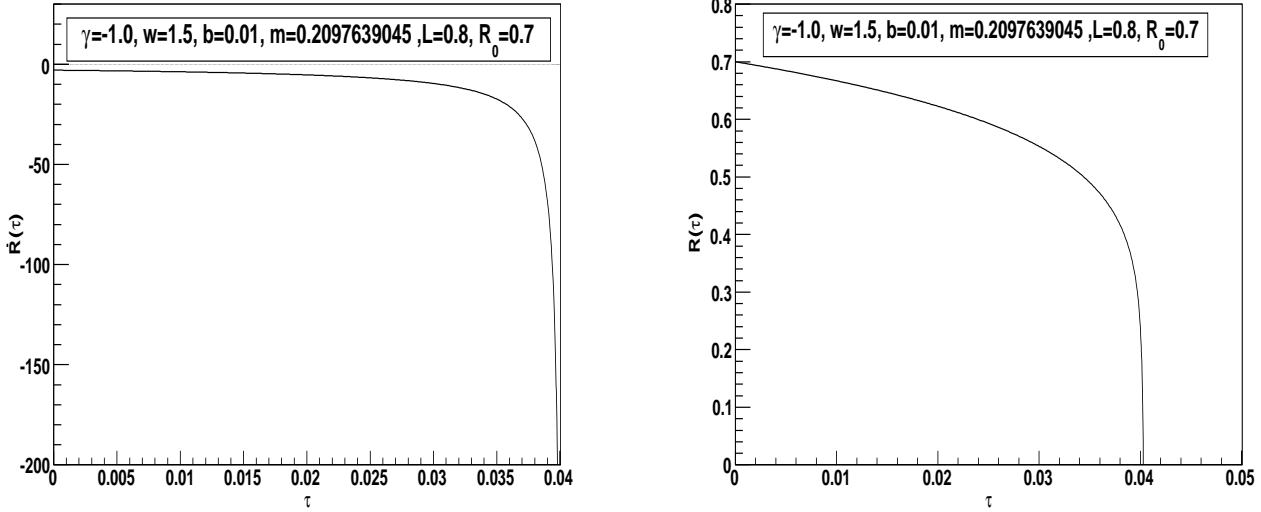


FIG. 2: These figures represent the dynamical evolution of the shell to a naked singularity for the potential given by the figure 1, assuming $R_0 = R(0) = 0.7$.

TABLE V: This table show the calculated horizons using the equations 28 and 29. The symbol $i = \sqrt{-1}$ denotes the imaginary constant. See figure 3.

m	L_e	Cosmological Horizon	Black Hole Horizon
0.3775	1.5	0.8943821768+0.3869863502 i	0.8943821767-0.3869863502 i
	L_e^*		
	1.97	1.1976796420	1.0759952780
	2.0053430150	1.2948106450	1.0151227670
	3	2.5081539280	0.8151917235
	20	19.61123828	0.7560805420
	∞	∞	2m=0.7550

- Brazil (Ref. 2399/03).

- [1] D. Horvat and S. Ilijic, arXiv:0707.1636; P. Marecki, arXiv:gr-qc/0612178; F.S.N. Lobo, Phys. Rev. D **75**, 024023 (2007); arXiv:gr-qc/0612030; Class. Quantum Grav. **23**, 1525 (2006); F.S.N.

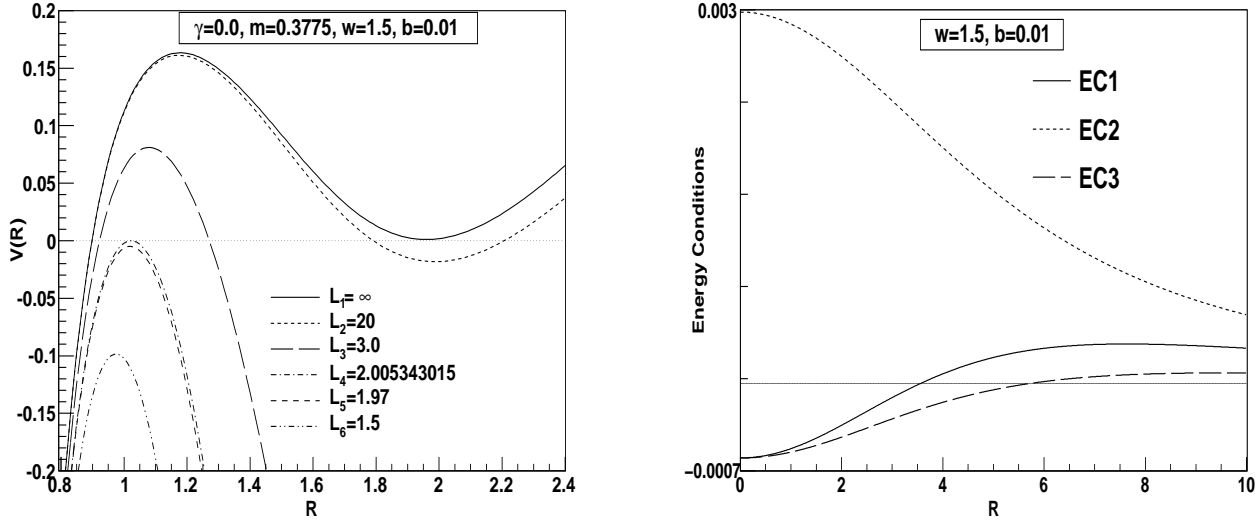


FIG. 3: The potential $V(R)$ and the energy conditions $EC1 \equiv \rho + p_r + 2p_t$, $EC2 \equiv \rho + p_r$ and $EC3 \equiv \rho + p_t$, for $\gamma = 0$, $\omega = 1.5$, $b = 0.01$ and $m_c = 0.3775$. **Case G**

TABLE VI: This table show the calculated horizons using the equations 28 and 29. The symbol $i = \sqrt{-1}$ denotes the imaginary constant. See figure 5.

m	L_e	Cosmological Horizon	Black Hole Horizon
0.2552945103	1.0	$0.5973628039 + 0.2655691220 i$	$0.5973628039 - 0.2655691220 i$
	L_e^*		
	1.36	0.8837041274	0.6823811248
	1.430886	1.002124260	0.6365867478
	1.6	1.220128096	0.5913790740
	12	11.73606139	0.5115184600
	∞	∞	$2m = 0.5105890206$

Lobo, Aaron V. B. Arellano, *ibid.*, **24**, 1069 (2007); T. Faber, arXiv:gr-qc/0607029; C. Cattoen, arXiv:gr-qc/0606011; O.B. Zaslavskii, Phys. Lett. **B634**, 111 (2006); C. Cattoen, T. Faber, and M. Visser, Class. Quantum Grav. **22**, 4189 (2005).

[2] E.J. Copeland, M. Sami and S. Tsujikawa, Int. J. Mod. Phys. **D15**, 1753 (2006); T. Padmanabhan, arXiv:07052533.

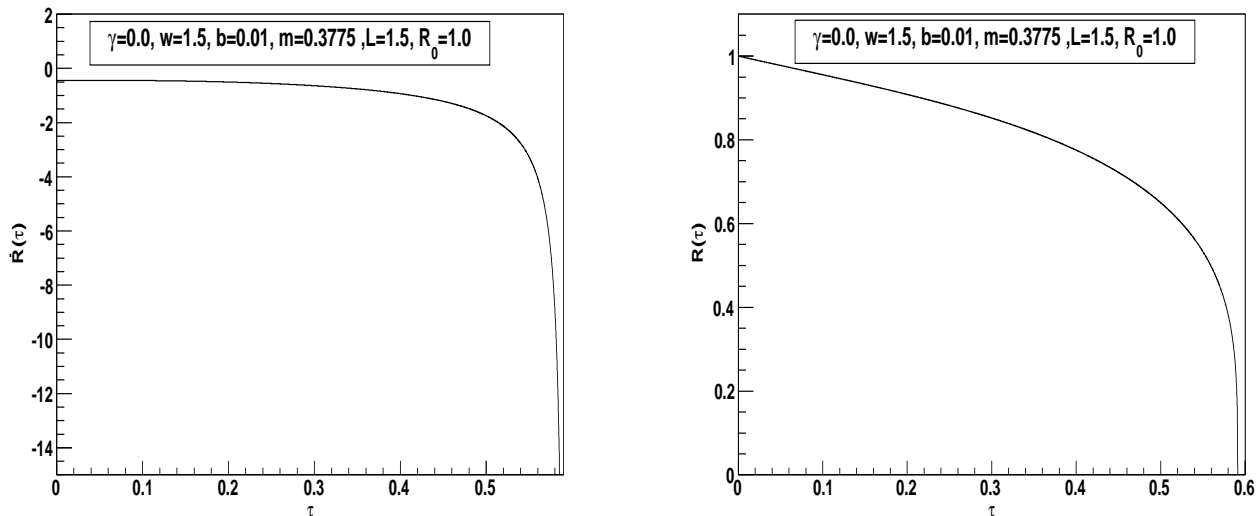


FIG. 4: These figures represent the dynamical evolution of the shell to a naked singularity for the potential given by the figure 3, assuming $R_0 = R(0) = 1$.

- [3] A.E. Broderick and R. Narayan, *Class. Quantum Grav.* **24**, 659 (2007) [arXiv:gr-qc/0701154].
- [4] P.O. Mazur and E. Mottola, ” *Gravitational Condensate Stars: An Alternative to Black Holes,*” arXiv:gr-qc/0109035; *Proc. Nat. Acad. Sci.* **101**, 9545 (2004) [arXiv:gr-qc/0407075].
- [5] Dymnikova I and Galaktionov E, ” *Vacuum Dark Fluid*”, *Physics Letters B* **645**,358 (2007) and references herein.
- [6] M. Visser and D.L. Wiltshire, *Class. Quantum Grav.* **21**, 1135 (2004)[arXiv:gr-qc/0310107].
- [7] B.M.N. Carter, *Class. Quantum Grav.* **22**, 4551 (2005) [arXiv:gr-qc/0509087].
- [8] A. DeBenedictis, *et al*, *Class. Quantum Grav.* **23**, 2303 (2006) [arXiv:gr-qc/0511097].
- [9] C.B.M.H. Chirenti and L. Rezzolla, arXiv:0706.1513.
- [10] P. Rocha, A.Y. Miguelote, R. Chan, M.F. da Silva, N.O. Santos, and A. Wang, ” *Bounded excursion stable gravastars and black holes,*” *J. Cosmol. Astropart. Phys.* **6**, 25 (2008) [arXiv:gr-qc/08034200].
- [11] P. Rocha, R. Chan, M.F. da Silva and A. Wang, ” *Stable and ”Bounded Excursion” Gravastars, and Black Holes in Einstein’s Theory of Gravity,*” *J. Cosmol. Astropart. Phys.* **11**, 10 (2008) [arXiv:gr-qc/08094879].
- [12] R. Chan, M.F. da Silva, P. Rocha and A. Wang, ” *Stable Gravastars with Anisotropic Dark*

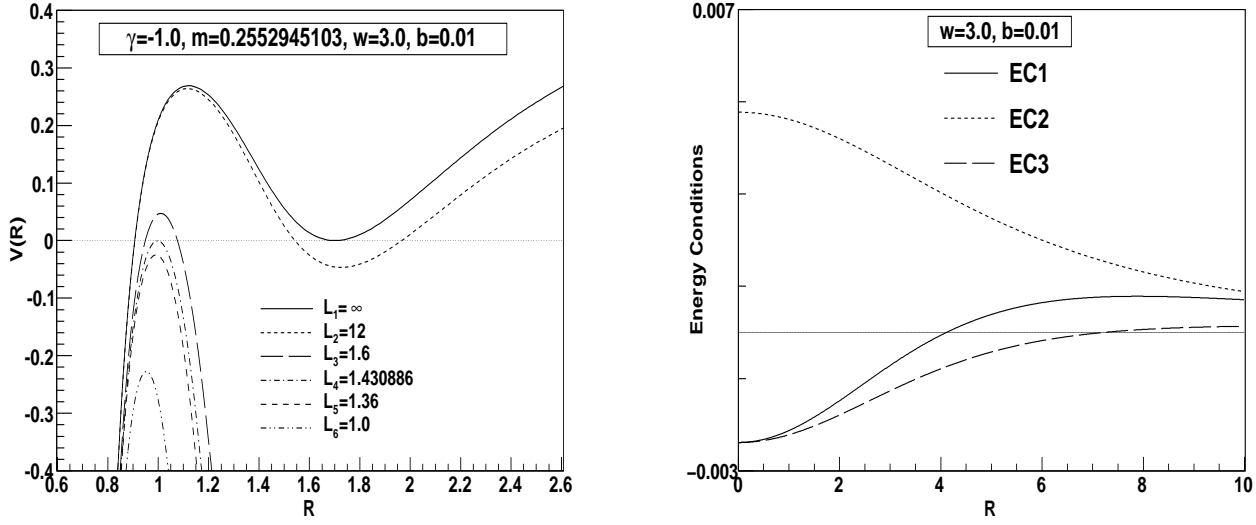


FIG. 5: The potential $V(R)$ and the energy conditions $EC1 \equiv \rho + p_r + 2p_t$, $EC2 \equiv \rho + p_r$ and $EC3 \equiv \rho + p_t$, for $\gamma = -1$, $\omega = 3$, $b = 0.01$ and $m_c = 0.2552945103$. **Case G**

Energy", J. Cosmol. Astropart. Phys. **3**, 10 (2009) [arXiv:gr-qc/08124924].

[13] R. Chan, M.F.A. da Silva and P. Rocha, "How the cosmological constant affects gravastar formation," J. Cosmol. Astropart. Phys. **12**, 17 (2009) [arXiv:gr-qc/09102054].

[14] R. Chan and M.F.A. da Silva, "How the charge can affect the formation of gravastars," J. Cosmol. Astropart. Phys. **7**, 29 (2010) [arXiv:gr-qc/10053703].

[15] R. Chan, M.F.A. da Silva, J.F. Villas da Rocha, "Star Models with Dark Energy" (2008) [arXiv:gr-qc/08033064]

[16] Bertolami, O., Páramos, J., Phys. Rev. D **72**, 123512 (2005) [arXiv:astro-ph/0509547]

[17] Lobo, F. (2007) [arXiv:gr-qc/0611083].

[18] Cattoen, C., Faber, T. and Visser, M. Class. Quantum Grav. **22** 4189 (2005).

[19] Dzhunushaliev V, Folomeev V , Myrzakulov R and Singleton D,"Non-singular solutions to Einstein-Klein-Gordon equations with a phantom scalar field", Journal of High Energy Physics **7**, 94 (2008), [arXiv:gr-qc/arXiv:0805.3211].

[20] Lobo, F., Class. Quant. Grav. **23**, 1525 (2006).

[21] Lake, K., Phys. Rev. D **19**, 2847 (1979).

[22] S.W. Hawking and G.F.R. Ellis, *The large scale structure of space-time* (Cambridge University

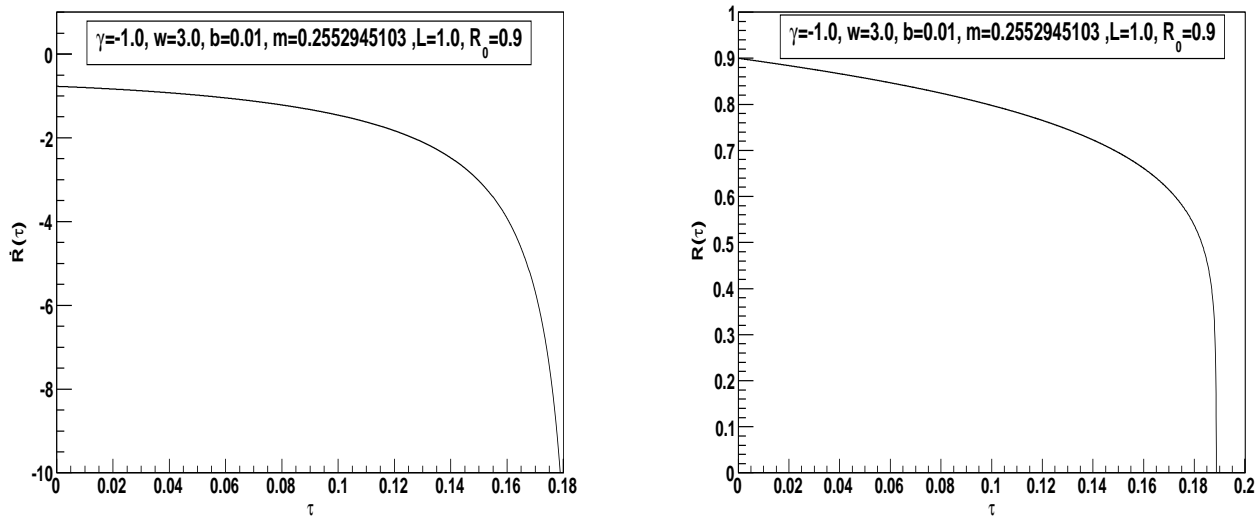


FIG. 6: These figures represent the dynamical evolution of shell to a naked singularity for the potential given by the figure 5, assuming $R_0 = R(0) = 0.9$.

Press, Cambridge, 1973).

[23] Chan, R., da Silva, M.F.A., Villas da Rocha, J.F., MPLA **24**, 1137, (2009).

[24] S. Shankaranarayanan, Phys. Rev. D. **67**, 084026 (2003).

[25] C. F. C. Brandt, Chan, R., da Silva, M.F.A., Villas da Rocha, J.F., IJMPD **19**, 317, (2010).